Non-Linear Autoregressive Delay-Dependent INS/GPS Navigation System Using Neural Networks

Mohammad Abdel Kareem Jaradat and Mamoun F. Abdel-Hafez

***Abstract*— Autoregressive neural network fusion architecture is presented for low-cost global positioning system (GPS) and inertial measurement unit (IMU) measurements integration. The proposed intelligent fusion architecture is a non-linear method that takes into account the variable delay between GPS measurement epochs. This delay is due to possible operation of the GPS/IMU integrated system in urban canyon environments. To verify the performance of the proposed method, a simulation environment is constructed. In the simulation environment, the vehicle's truth model is known and GPS/IMU measurements are simulated with a number of GPS measurements outages. The performance of the proposed fusion architecture is evaluated against the truth state of the vehicle. Subsequently, the proposed method is used in an experimental setup to estimate the state of a vehicle that is driven through a number of chosen paths. The performance of the fusion architecture is compared against a commercial off-the shelf solution.**

***Index Terms*— Navigation, intelligent nonlinear sensor fusion, INS/GPS integration, nonlinear autoregressive neural network.**

I. Introduction

With the increase in autonomy in vehicular/transportation industry, researchers continue to work on improvements in the design of aided inertial navigation systems (INS) [1]–[5]. Due to the integrity of GPS signals, GPS aided INS systems are the main solution used in many applications [5]–[7]. The main reason behind this is that the error in the GPS solution does not grow with time. This is contrary to the error propagation in the INS solution which is based on integrating the IMU measured vehicle kinematics. The error in the INS velocity and attitude estimates grows linearly while the INS position error grows quadratic with time [8], [9].

Utilizing GPS/IMU systems in the autonomy of vehicular systems have increased with the increase in the market demand for autonomous vehicles. For air vehicle systems, high accuracy estimates is obtained from GPS/IMU systems. This is due to the continuous availability of the required minimum number of satellites in the line of view of the GPS system [10], [11]. At the same time, the possible measurement fault or quality degradation in the GPS/IMU system has to be monitored [12]–[14]. However, for ground vehicles, usual operation in urban canyon environments limits the ability to continuously acquiring the GPS signal [15]–[17]. Therefore, GPS signal blockage has to be taken into account in the fusion of the GPS/IMU measurements. Additionally, the uncertainty in the delay time between GPS measurements due to this blockage have to also be accounted for in the fusion algorithm.

Another challenge in the utilization of GPS/IMU systems for ground vehicles is the allowable systems cost [18], [19]. In air vehicle systems, high-accuracy GPS/IMU systems can be utilized. However, competition in marketable ground vehicles constrains the utilization of high-quality GPS/IMU systems. Instead, low-cost, commercial of-the-shelf (COTS) sensors have to be used. These COTS sensors are characterized by lower measurement accuracy [19]. Therefore, these low-quality measurements have to be taken into account in the utilized sensor fusion algorithm [20]–[22].

The fusion of GPS/IMU sensors is commonly approached using mechanistic models. Most of these approaches are Kalman-based filters [23]. As the GPS/IMU kinematic model is non-linear, a linearization step has to be first performed before implementing the fusion algorithm. Therefore, an error state between the true vehicle state and the linearization state is produced [24]. The filter is used to estimate this error and subsequently the estimate is added to the nominal vehicle state to produce the updated estimate of the vehicle.

If the error between the true vehicle state and the nominal linearization state is large, the linearized filters are known to diverge from the true estimate [25]. Therefore, nonlinear sensor fusion algorithms need to be utilized. The use of low-cost GPS/IMU sensors dictates the design of conservative estimators that take into account possible increase in the state estimation error. Among the nonlinear estimators that are commonly used to compensate for this possible error are intelligent fusion techniques [5], [26]–[37].

Fuzzy logic, neural networks, or hybrid integrated approaches are considered the most newfangled approaches among the developed intelligent approaches to enhance GPS/INS nonlinear integration [38]. However, the main idea of the proposed approaches is to provide an estimate to the vehicle dynamics. This estimation is generally based on the GPS signal using the modeled error dynamics of the INS sensor represented by general neural networks or hybrid neuro-fuzzy systems [37], [38]. These techniques relate INS errors to INS output at specific time intervals only. The input

Manuscript received June 24, 2016; revised October 25, 2016; accepted December 5, 2016. Date of publication December 20, 2016; date of current version January 19, 2017. The associate editor coordinating the review of this paper and approving it for publication was Prof. Alexander Fish.

M. A. Jaradat is with the Department of Mechanical Engineering, Jordan University of Science and Technology, Irbid, Jordan, and also with the Department of Mechanical Engineering, American University of Sharjah, Sharjah, United Arab Emirates.

M. F. Abdel-Hafez is with Department of Mechanical Engineering, American University of Sharjah, Sharjah, United Arab Emirates.

Digital Object Identifier 10.1109/JSEN.2016.2642040

delayed neural networks have been proposed to overcome time dependency problems, the INS position and velocity errors were modeled based on the current and the past INS position and velocity data [5], [38]. This neural network approach is mainly utilizing a dynamic sliding window. It is considered more reliable in representing the system's dynamics. However, it also increases the amount of network complexity. On the sequel, the training time will increase based on the selected network architecture and the selected input features [5].

From previous literature, navigation systems can be categorized into conventional linear fusion systems such as those utilizing Kalman Filters [1]–[4], [6], [12], [13], [17], [27], [29], and nonlinear fusion systems which utilize Extended Kalman Filters and intelligent fusion techniques [5], [7]–[11], [14]–[17], [20], [23], [26], [28], [30]–[34], [38]. Among the latter, in reference [5], the possibly varying delay between the availability of GPS measurements was considered within the fusion technique as an input. The measurements were fused utilizing adaptive-neuro-fuzzy system, targeting better state estimation compared to previous approaches.

In this paper, an intelligent fusion technique is proposed for low-cost GPS/IMU measurements fusion. The proposed algorithm is based on a non-linear autoregressive intelligent fusion technique, mainly using additive nonlinear autoregressive exogenous (ANARX) models. The developed integrated navigation solution proposes neural networks implementation of additive nonlinear autoregressive exogenous (ANARX) models on nonlinear discrete time system. The solutions aims at achieving an optimal integration utilizing the available information from the sensors and its time of availability. The possibly varying delay between the availability of GPS measurements is taken into account in the fusion technique. This is done to account for possible operation of the system during, varying-magnitudes, GPS outages. The technique is incorporated on a low-cost navigation system that is used to demonstrate the performance of the measurement fusion accuracy in real-time experiments. As the outage of GPS measurements increases, the error in the estimate, based on a linearized system mode, increases. This is why the proposed scheme utilizes a non-linear autoregressive intelligent fusion technique to enhance the accuracy of the state estimate.

In the proposed navigation system, a low-cost GPS receiver measures the position of the vehicle at a low frequency of 5 Hz. Three-axis accelerometers and gyroscopes measure the linear acceleration and angular velocity of the vehicle at a frequency rate of 50 Hz. The results obtained for the new proposed approaches are verified against a commercial off-the-shelf (COTS) MIDG solution [39]. Using measurements from the GPS receiver, the IMU three-axis acceleration measurement and the IMU three-axis angular velocity measurements are integrated to obtain the position and velocity of the vehicle at 50 Hz [39]. These INS estimates are used as inputs to the proposed fusion technique.

The layout of this paper is as follows. In Section II, the algorithm to obtain the vehicle kinematics is described. The methodology of fusing the IMU/GPS measurements using the delay-dependent, non-linear, autoregressive technique is illustrated in section III. The simulation environment that is used to validate the performance of the proposed technique is given in section IV. The simulation results are also shown in section IV. Experimental validation of the proposed technique is presented in Section V. Finally, concluding remarks are given in Section VI.

II. Propagated Vehicle Kinematics

Given the initial position, velocity, and attitude of the vehicle, the measured acceleration of the vehicle can be integrated to obtain the variation of the position and velocity of the vehicle with time. Simultaneously, the measured angular acceleration of the vehicle has to be integrated to obtain the variation of the attitude of the vehicle with time. These vehicle kinematics are subsequently used to control the vehicle along a desired trajectory [24].

The fact that the vehicle's measured acceleration and angular velocity are biased, limits the accuracy of the integrated vehicle's state. Additionally, the initial position, velocity and attitude of the vehicle do not necessary represent the true initial state of the vehicle. Therefore, aiding sensors have to be used to correct the propagated estimates of the vehicle's state [25].

In this work, we use an IMU to measure the specific force of the vehicle, $\mathrm{F^b}$. The used IMU is a strap-down type which measures the vehicle's specific force in the vehicle's body frame along three perpendicular axes. Similarly, the IMU measures the angular velocity of the vehicle, ω^{b}, along three perpendicular body frame axes. These measurements are used to obtain the dynamic model of the system.

The vehicle kinematics can be derived starting with the position of the vehicle relative to the inertial frame, represented as:

$$P|_I = \mathrm{C_E^I} P|_E \tag{1}$$

Where $P|_I$ is the position of the vehicle relative to the inertial frame, $\mathrm{C_E^I}$ is the cosine rotation matrix from the Earth-centered, earth-fixed frame (ECEF) to the inertial frame, and $P|_E$ is the position of the vehicle relative to the ECEF frame.

Differentiating equation 1 with respect to time, we get:

$$V|_I = \mathrm{C_E^I} V|_E + \omega_E^I \times \mathrm{C_E^I} P|_E \tag{2}$$

Where $V|_I$ is the velocity of the vehicle with respect to the inertial frame, $V|_E$ is the velocity of the vehicle with respect to the ECEF frame, and ω_E^I is the angular velocity of the ECEF with respect to the inertial frame.

Differentiating equation (2) with respect to time we get:

$$\dot{V}|_I = \mathrm{C_E^I} \dot{V}|_E + 2\omega_E^I \times \mathrm{C_E^I} V|_E + \omega_E^I \times \omega_E^I \times \mathrm{C_E^I} P|_E \tag{3}$$

Where, $\dot{V}|_I$ is acceleration of the vehicle with respect to the inertial frame and $\dot{V}|_E$ is the acceleration of the vehicle with respect to the ECEF frame. However, the absolute acceleration is related to the measurement of the strapdown accelerometer by:

$$\dot{V}|_I = \mathrm{F^b} + G \tag{4}$$

where, G is the gravitational acceleration. Therefore, when representing all variable in the ECEF frame, the variation of the velocity of the vehicle with respect to the ECEF is related to the measured body-frame vehicle's specific force as [12]:

$$\dot{V}^{\mathrm{e}} = \mathrm{C_B^E F^b} - 2\Omega \mathrm{V^e} - \Omega^2 \mathrm{P^e} + \mathrm{G^e} \tag{5}$$

where, $V^e = \dot{V}|_E$ is the velocity of the vehicle with respect to the ECEF frame, C_B^E is the cosine rotation matrix from the body frame to the ECEF frame, $\Omega = [\omega_E^I \times]$ is the skew-symmetric matrix of the angular velocity of earth with respect to the ECEF frame, $P^e = P|_E$ is the vehicle's position represented in the ECEF frame, and G^e is the gravitational acceleration represented in the ECEF frame. Please note that the small letter superscript in the equation 1, and in the equations to follow, denotes the representation of a vector in a certain coordinate frame. For example, F^b denotes that the specific force is measured in the vehicle's body frame and V^e denotes that the velocity of the vehicle is represented in the ECEF frame. The term on the right side of equation (5) represents the Coriolis acceleration.

Equation 5 is integrated to obtain the velocity of the vehicle and subsequently integrated again to obtain the position of the vehicle. Nevertheless, as mentioned above, the obtained velocity and position are biased from the true vehicles' velocity and position. This is a result of the error, measurement noise and bias, in the vehicle's measured acceleration and angular velocity. The measured vehicle's specific force $\hat{F}^b$ is related to the true vehicle's specific force F^b as:

$$\hat{F}^b = F^b - b_a^b - w_a \tag{6}$$

where, b_a^b is the IMU accelerometer's bias represented in the vehicle's body frame and w_a is the accelerometer's noise which is assumed as a Gaussian white noise.

The vehicle's attitude with respect to the ECEF is represented in quaternion format as [12]:

$$q_{eb}^e = \begin{bmatrix} q_0 \\ q_1 \\ q_2 \\ q_3 \end{bmatrix} \tag{7}$$

the variation of this attitude with respect to time is given as [12]:

$$\dot{q}_{eb}^e = \frac{1}{2}\Omega_{eb}^b q_{eb}^e \tag{8}$$

where, Ω_{eb}^b is the skew-symmetric matrix of the angular velocity of the vehicle relative to the ECEF frame. If the angular velocity of the vehicle with respect to the ECEF frame is represented as:

$$\omega_{eb}^b = \begin{bmatrix} \omega_x \\ \omega_y \\ \omega_z \end{bmatrix} \tag{9}$$

then Ω_{eb}^b is given as:

$$\Omega_{eb}^b = \begin{bmatrix} 0 & -\omega_x & -\omega_y & -\omega_z \\ \omega_x & 0 & \omega_z & -\omega_y \\ \omega_y & -\omega_z & 0 & \omega_x \\ \omega_z & \omega_y & -\omega_x & 0 \end{bmatrix} \tag{10}$$

However, the used strap-down IMU measures the angular velocity of the vehicle relative to the inertial frame, ω_{ib}^b. Therefore, ω_{eb}^b is obtained by subtracting the angular velocity of earth relative to the inertial frame, ω_{ie}^e, as:

$$\omega_{eb}^b = \omega_{ib}^b - C_E^B \omega_{ie}^e \tag{11}$$

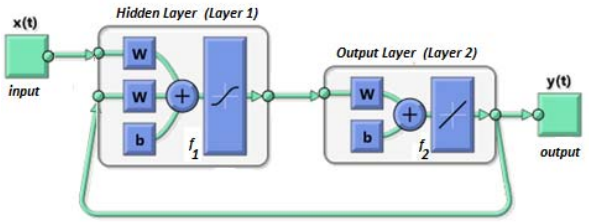

Fig. 1. General architecture of feedforward neural network additive nonlinear autoregressive with exogenous external input (ANARX) model.

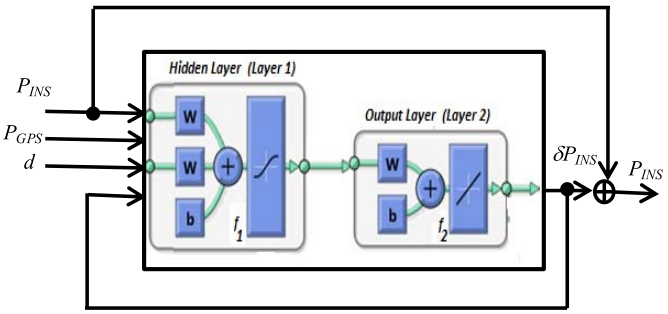

Fig. 2. General architecture of navigation solution using ANARX network.

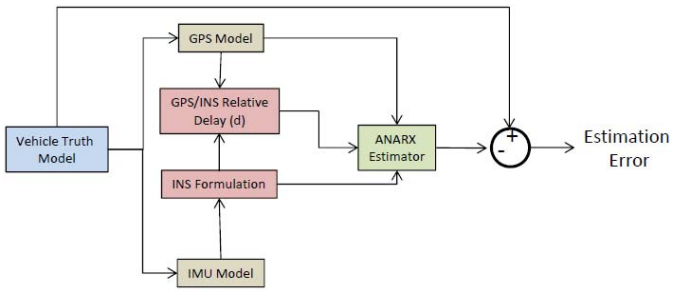

Fig. 3. GPS/INS simulation environment block diagram.

Therefore, equation 8 is integrated to obtain the attitude of the vehicle throughout its trajectory of motion. However, the IMU measured angular velocity of the vehicle is biased from the vehicle's true angular velocity. This will cause an error in the obtained vehicle's attitude. Additionally, this error will be increasing in time. The bias in the angular velocity measurement is seen in the measurement equation as:

$$\hat{\omega}_{ib}^b = \omega_{ib}^b - b_g^b - w_g \tag{12}$$

where, $\hat{\omega}_{ib}^b$ is the IMU measured angular velocity of the vehicle, ω_{ib}^b is the true angular velocity of the vehicle, b_g^b is the bias on the angular velocity measurement, and w_g is the noise error on the angular velocity measurement. The measurement noise, w_g, is assumed as a Gaussian white noise process. All of these variables are represented in the body frame.

From the above discussion, we see that the two, possibly time-varying, bias sequences in equations 6 and 12 will cause an error in the obtained vehicle kinematics. Additionally, the error in the propagated vehicle kinematics will increase with time. Therefore, an aiding sensor has to be utilized to eliminate this error. In this work, the GPS measurements are used for this purpose.

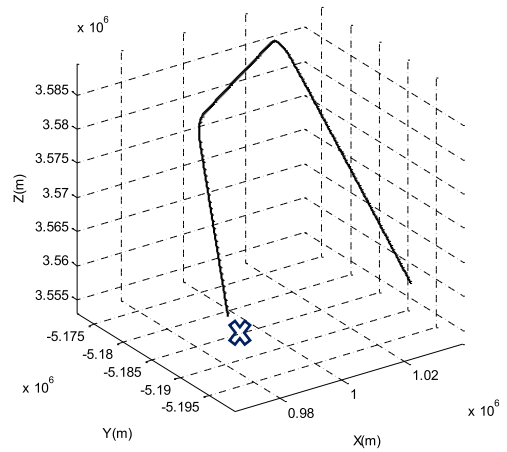

Fig. 4. The traveled path by the vehicle during the conducted simulation scenario in the x, y and z directions. The starting point denoted by x.

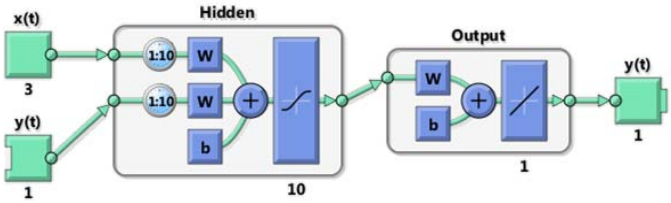

Fig. 5. Open loop ANARX model in the x, y and z directions.

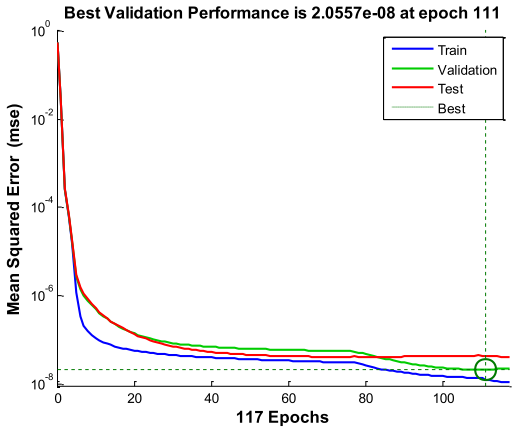

Fig. 6. The mean squared error (MSE) for the open loop ANARX model in the x direction during the training phase.

Low-cost GPS measurements are sampled at a much slower rate than the IMU measurements. As an example, the system developed in this work samples the IMU at 50 Hz while the GPS is sampled at 5Hz. The more the delay between successive GPS measurements, the more error will accumulate on the integrated vehicle kinematics. The problem gets more complicated when the GPS measurements are missed due to blockage or due to loss of receiver's lock on the signal.

A fusion technique has to be applied to provide a high-accuracy vehicle's state estimate. The fusion technique should take account for the possibly varying delay between the IMU and GPS measurements. Since the kinematic relations of the system given in equations 5-12 are non-linear, we propose the use of a delay-dependent, non-linear, autoregressive method to fuse the measurements from the IMU and GPS.

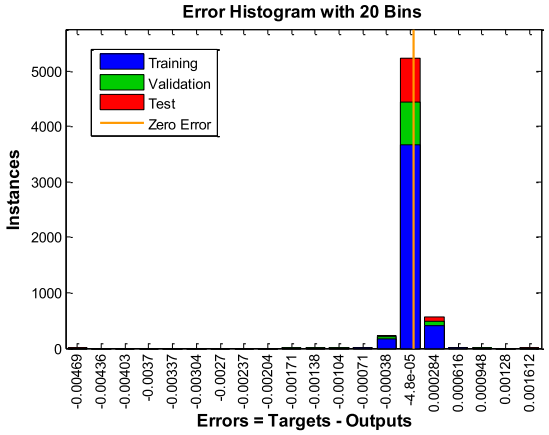

(a)

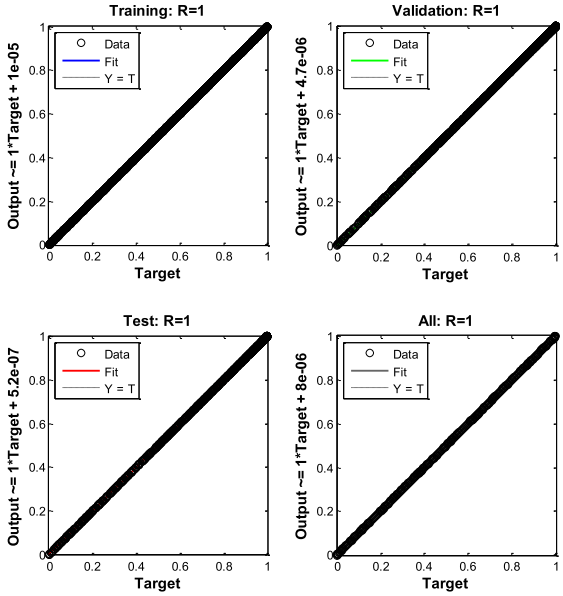

(b)

Fig. 7. The performance of the open loop ANARX model in the x direction after the training phase: (a) error histogram and (b) validation of the model performance with respect to: training data, validation data, test data and all that data, respectively.

III. INS/GPS Integration

The developed integrated navigation solution depends on neural networks implementation of additive nonlinear autoregressive exogenous (ANARX) models to nonlinear discrete time system.

Based on the NARX model the output y mainly estimated using the nonlinear function f(t) which in turn depends on the previous outputs and the set of independent inputs u [40]–[42]:

$$y(t+1) = f(Y(m), U(n)) \tag{13}$$

where Y(m)= [y(t) y(t-1) …y(t-m)], U(n)= [u(t) u(t-1) …u(t-n)] and n ≤m. The proposed system will precede the error in the INS solution (δPINS) based on the availability of the GPS measurements (P_{GPS}), the INS measurements (P_{INS}),

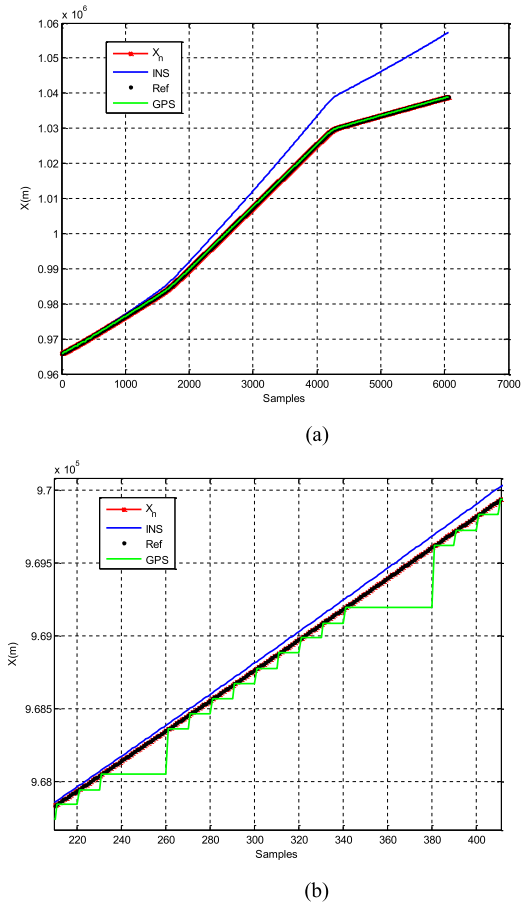

Fig. 8. The fused data along the x direction (a) the whole trajectory in the x direction (b) a zoomed part of the trajectory.

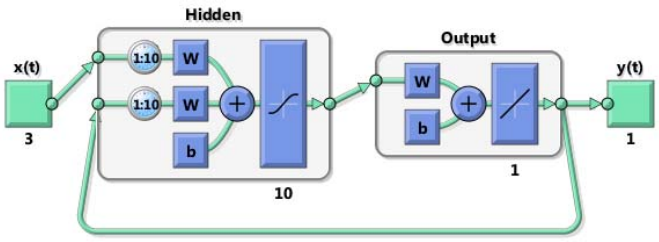

Fig. 9. Closed-loop ANARX model in the x, y and z directions.

and number of INS integration steps (d) since the last GPS reading. This number results from the differences between the INS and the GPS sampling rates and the possible missed, or blocked, GPS readings.

For neural networks implementation, the NARX model can be represents as additive nonlinear model, ANARX model [40], [41]:

$$\delta P_{INS}\,(t+1) = \sum_{i=1}^{n} f_i(\delta P_{INS_{t-i}}, u_{t-i}) \qquad (14)$$

where f_i is a nonlinear smooth function and the set of independent inputs u_t consists of the measurements $[P_{INS} P_{GPS} d]$. Generally equation (14) can be represented by two layer feedforward neural networks; schematic is shown in figure (1) [42]. Using neural network notations, the network output is defined

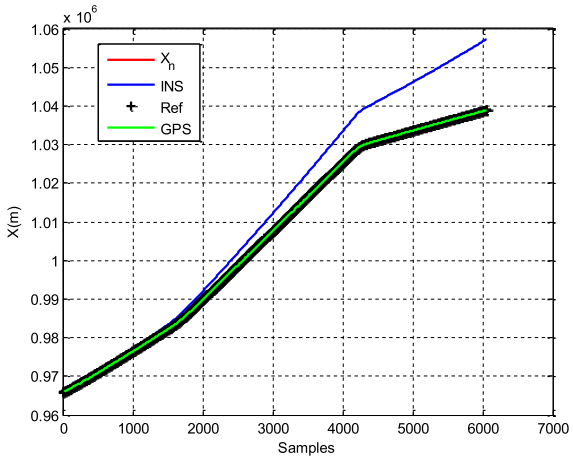

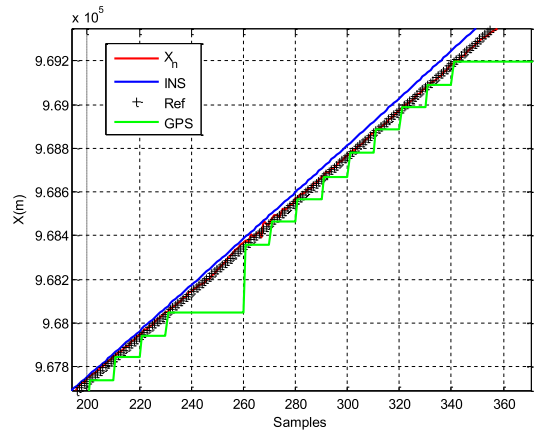

Fig. 10. The fused data along the x direction using closed loop model (a) the whole trajectory along the x direction (b) a zoomed part of the trajectory.

by [40], [41]:

$$\delta P_{INS}\,(t+1) = \sum_{i=1}^{n} W_i^2 f_i(W_i^1[\delta P_{INS_{t-i-1}}, u_{t-i-1}]) \qquad (15)$$

For the represented feedforward neural networks W_i^2 and W_i^1 are the weights matrices for the first and second layer, respectively. Additionally, f_i is a nonlinear smooth saturation function selected as a sigmoid and a linear transfer function for the hidden and the output layers, respectively [40]–[42]. If the GPS measured position is not available, then the proposed ANARX network, which characterizes the error dynamics (δP_{INS}), is used to correct the INS position as in figure (2). The developed integrated INS/GPS navigation solution depends on neural networks implementation of ANARX models to nonlinear discrete time system, as follows:

$$P'_{INS}(t+1) = P_{INS}\,(t+1) + \sum_{i=1}^{n} W_i^2 f_i(W_i^1[\delta P_{INS_{t-i-1}}, u_{t-i-1}]) \qquad (16)$$

where P'_{INS} is the corrected INS position based on the INS sensor's estimated error dynamics (δPINS). The last right-side

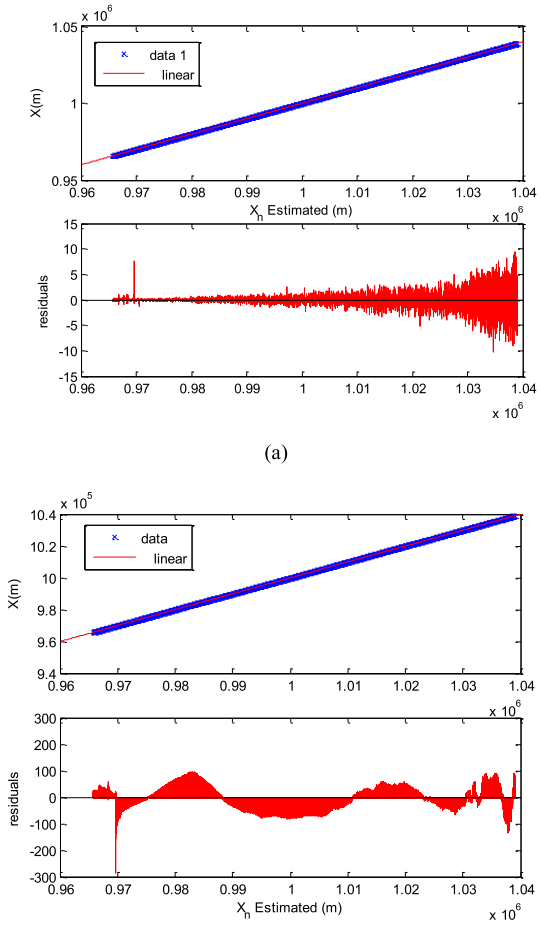

Fig. 11. The fused data scatter plot vs. actual data along the x direction using (a) open loop and (b) closed-loop models.

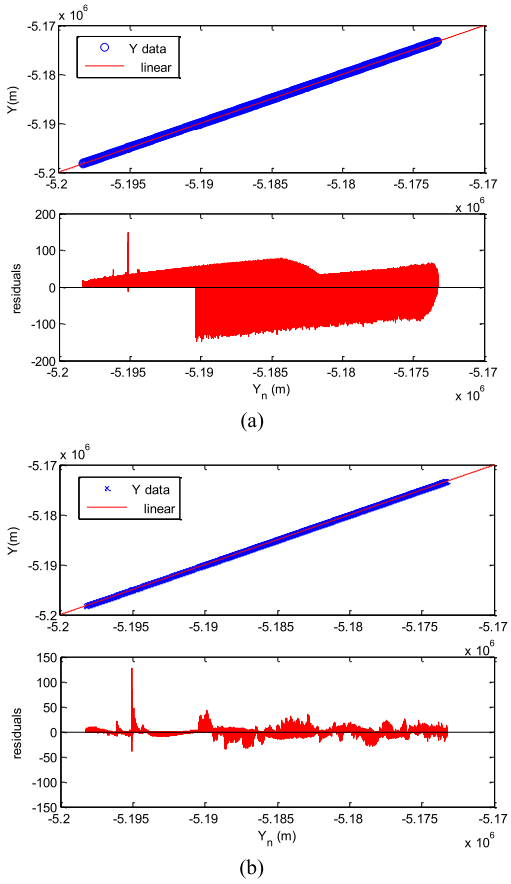

Fig. 12. The fused data scatter plot vs. actual data along the y direction using (a) the open loop and (b) the closed-loop models.

term of equation (16) represents the ANARX estimated error dynamics due to the INS sensors (δPINS). After the training phase, ANARX network provides a nonlinear representation which describes the INS error dynamics based on the given set of inputs. In order to optimize the network weights matrices W_i^2andW_i^1 during the training phase, an optimization approach is utilized. Commonly, Levenberg Marquardt approach is adopted due to its efficiency and training speed. During the training phase, the ANARX network continues to tune its weights, such that the mean square error (MSE) is minimized [40]–[42]:

$$\mathrm{MSE} = \frac{1}{2m}\sum_{k=1}^{m}(Y_d(t) - Y_a(t))^2 = \frac{1}{2m}\sum_{k=1}^{m} e^2 \qquad (17)$$

where Y_d is the desired output at time t, Y_a is the network output at time t, and m is the total number of samples used during training phase. The gradient function is defined by [40]–[42]:

$$\delta = \frac{\partial \mathrm{MSE}}{\partial w} = J^T e \qquad (18)$$

where J is the Jacobian matrix which contains the network error derivative with respect to the adjustable network weight parameters. The Hessian matrix is defined as [40], [41]:

$$H = J(\nabla \mathrm{MSE}) = J^T J \qquad (19)$$

However, the adjustable parameters are optimized during the backward pass, while keeping them unchanged during the forward pass to find the network output, as [40], [41]:

$$w_{k+1} = w_k + \Delta w \qquad (20)$$

$$\Delta w = -(H + \mu I)^{-1}\delta \qquad (21)$$

where μ is the adaptive learning rate, and I is the identity matrix. A parallel architecture is developed to characterize each component of the INS position vector in the x, y, and z directions. Each subsystem is trained separately to achieve optimal performance by optimizing the network weights matrices during the training phase.

IV. Simulation Environment

The proposed algorithm was tested in a simulation environment [9], shown in Figure 3. In this environment, the vehicle truth state is known. Therefore, the true error in the position estimate can be calculated.

A linear specific force and angular velocity profiles were selected for the vehicle. The truth position, velocity, and attitude of the vehicle were obtained using equations (5-8). The IMU model in Figure 3 was used to simulate the measured IMU's specific force and angular velocity of the vehicle. A bias was simulated on these measurements as shown in equations (6, 12). The white noise driven biases on the specific force

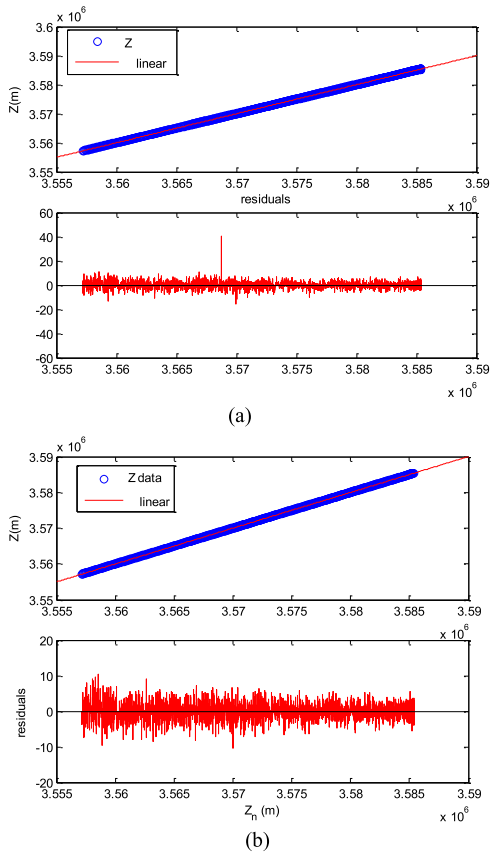

Fig. 13. The fused data scatter plot vs. actual data along the z direction using (a) the open loop and (b) the closed-loop models.

and angular velocity measurements are given as:

$$\dot{b}_{a}^{b} = w_{ba} \tag{22}$$

$$\dot{b}_{g}^{b} = w_{bg} \tag{23}$$

The vehicle's specific force bias and angular velocity bias affecting the IMU measurements were obtained by numerically integrating Equations (22) and (23). These biases were used in Equations (6) and (12) to simulate the IMU measurements. The INS state was then obtained by using the integrated biases in equations (5-8). This is represented in Figure 3 by the INS Formulation block.

The GPS position measurements were simulated from the true state of the vehicle. The noise on the GPS position measurements was simulated as an independent and identically-distributed (iid) Gaussian white noise process with zero mean and a standard deviation of 2 m. The zero-mean noise was assumed to reflect the use of differencing techniques to remove any GPS measurement bias [9], [13], [14]. This bias is a result of common GPS signal delay that is caused by inospheric errors, tropospheric errors, multipath, and clock errors. This process is shown in Figure 3 in the GPS model block.

The difference in the measurement sampling rate between the GPS and the IMU is simulated in the GPS/INS relative delay block of figure 3. Possible missed GPS epochs are also simulated in this block. Four GPS missed epochs were simulated during the scenario presented in this section.

The proposed approach was validated by applying the simulated sensors data to the developed ANARX system.

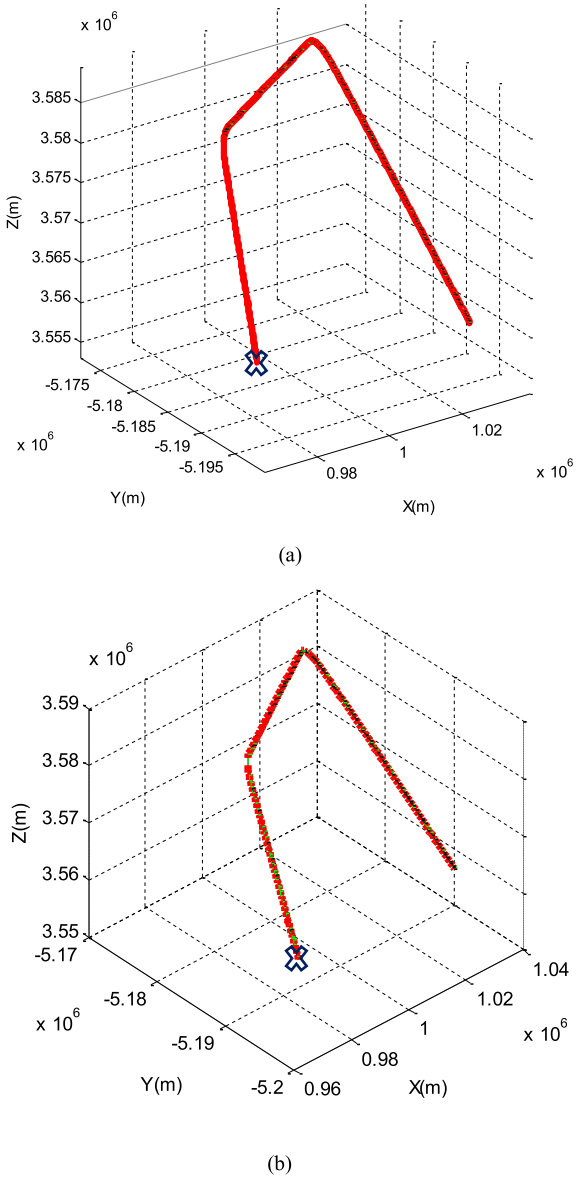

Fig. 14. The fused path using the proposed approach during the conducted simulation scenario in the x, y and z directions using (a) the open loop model and (b) the closed-loop model. The starting point denoted by x.

During this simulation scenario, the vehicle traveled along three dimensional path along x, y and z directions as demonstrated in figure 4.

Initially the ANARX open loop model was used during the training phase as shown in figure 5. The data was divided randomly into different sets to provide the intelligent knowledge by the system during the training phase, while the rest of the data sets were kept for validation and testing of the approaches. The performance for the developed ANARX training during the training phase is shown in figure 6. For better illustration, the error histogram and data regression plots for the different sets are shown in figure 7a, and 7b, respectively.

The estimated position in the x direction based on the proposed approach is demonstrated in figure 8. As can be noticed from the demonstrated results, the proposed approach provides excellent fusion for the position in the x direction.

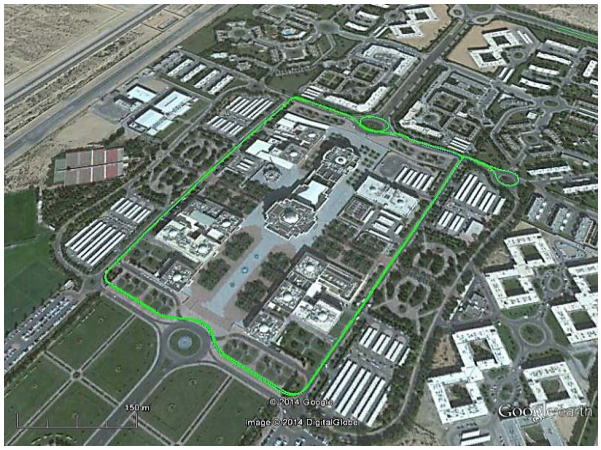

Fig. 15. Path driven by the vehicle during the data collection.

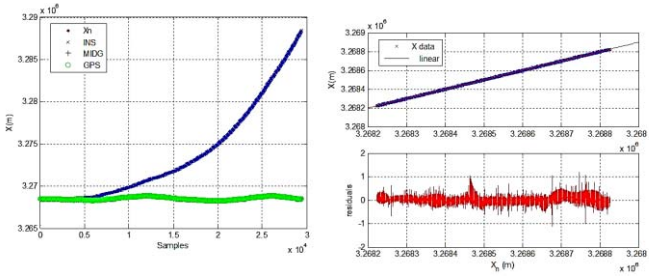

(a) (b)

Fig. 16. (a) The fused path along the x direction by the proposed approach. (b) The fused data scatter plot compared to the MIDG solution along the x direction using open loop ANARX model.

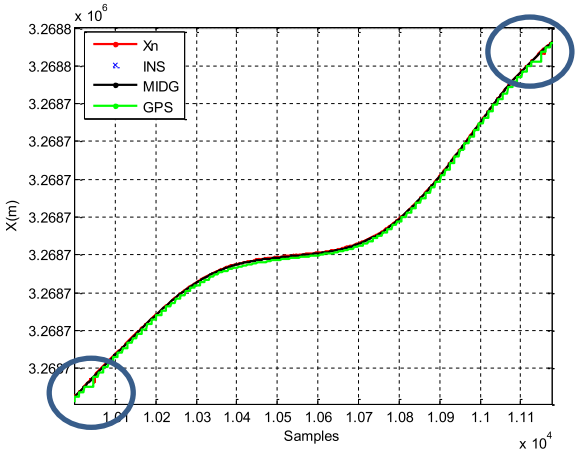

Fig. 17. The fused path along the x direction for selected period.

This performance was attained in spite of the INS signal drift as well as the GPS signal outages as clarified in figure 8b. Moreover, the difference in sampling frequency between the vehicle dynamics measured by the INS and the GPS receiver's position of the vehicle was completely handled.

For real time validation the closed loop model of the ANARX network proposed approach was implemented as shown in figure 9. In this model, the ANARX network completely depends on the feedback estimated values from the developed integration of the INS/GPS navigation systems

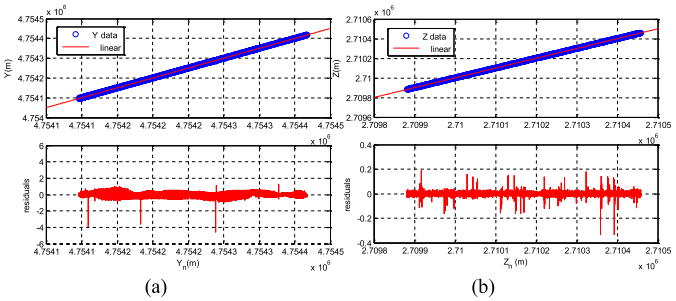

(a) (b)

Fig. 18. The fused data scatter plot along the y, and z directions using open loop ANARX model.

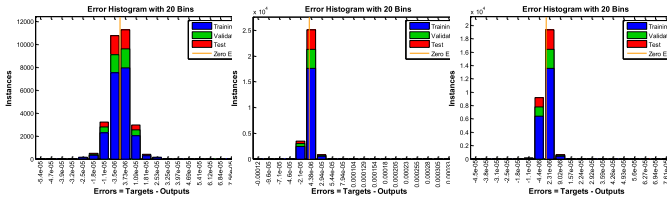

(a) (b) (c)

Fig. 19. The fused data error histogram plots along the x, y, and z directions after the training phase for the open ANARX model.

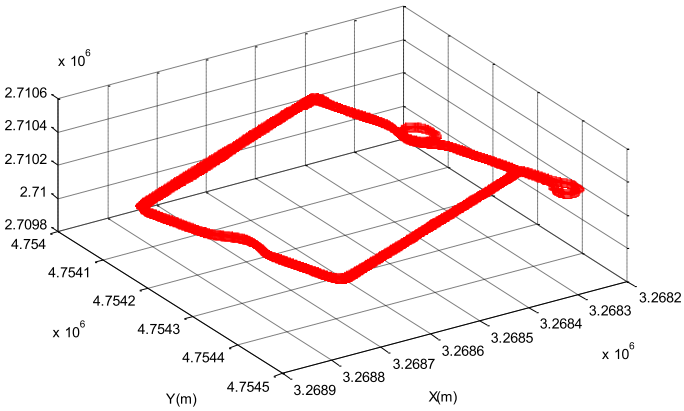

Fig. 20. Estimated vehicle position along the x, y and z directions using the proposed open ANARX model.

after training. No information is utilized from the actual target values, used during training, within this model.

The estimated position in the x direction based on the closed loop model for the proposed approach is demonstrated in figure 10. As can be noticed from the demonstrated results, the proposed closed loop approach provides excellent fusion for the position in the x direction in a similar trend as to the open loop model. As expected, an excellent performance was attained in spite of the INS signal drift. Moreover, the difference in sampling frequency between the vehicle dynamics measured by the INS and the GPS receiver's position of the vehicle was completely handled. Additionally, the GPS signal outages was successfully compensated for during the closed loop model, as clarified in figure 10b. For better demonstration of the comparison between the two models, the fused data scatter plots along the x direction is shown in Figure 11. The residual subplots demonstrated the proposed system's performance in correcting the estimated position based on the given inputs and availability of the output from the developed ANARX network.

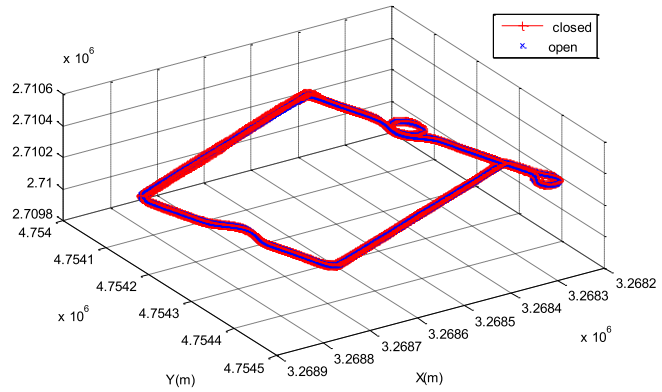

Fig. 21. Estimated vehicle position along the x, y and z directions using the proposed closed ANARX model.

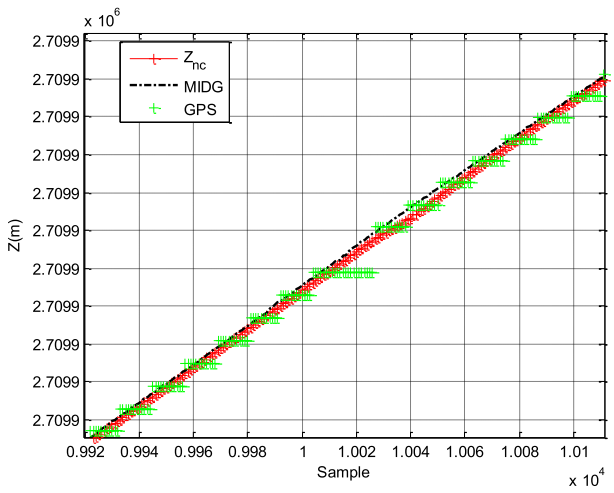

Fig. 22. Zoomed part of the fused data along the z direction using closed mode model.

The same procedure was applied to fuse the simulated vehicle position in the y and z directions. The fused data scatter plots along the y and z directions using the two models of the proposed approaches are shown in figures 12 and 13, respectively. The residual subplots demonstrated the ability of the proposed system to correct the estimated position based on the given inputs in y and z directions using the two models. An excellent performance was achieved in spite of the INS signal drift along these directions. Besides, the difference in sampling frequency between the vehicle dynamics measured by the INS sensor and the GPS receiver's position of the vehicle was completely handled along these directions. The complete fused path traveled during the conducted simulation scenario in the x, y and z directions using the two open loop and closed models is shown in Figure 14a and 14b respectively. As can be noticed, the estimated path utilizing the parallel structure of the proposed approaches completely agrees with the simulated path traveled during the conducted simulation scenario, see Figure 4.

V. Experimental Validation

The proposed approach was validated in a real time experiment. The data from the INS sensor and the GPS receiver was collected as the vehicle was driven along the path shown in Figure 15. This path is located within the premises of the American University of Sharjah (AUS). The measurements from the IMU unit were sampled at 50 Hz. A GPS sensor was used to correct the INS estimated position. This is due to drift in the INS state caused by the inherent IMU measurement biases [17]–[19]. The GPS was updated at a rate of 5 Hz during this experiment. The estimated track obtained from the proposed approach was validated against a commercial off-the shelf (COTS) MIDG solution [39].

The collected data from the INS/GPS sensors during the conducted drive test was used to train and validate the proposed approach. The data was divided randomly into three different sets. One set was used for training, while others two sets were kept for approach validation and testing. Figures 16 a shows the results of the fused estimate after applying the collected data to the proposed approach in the x direction, plotted compared to the MIDG solution using the open loop mode during the training phase. The residual subplot, shown in figure 16b, demonstrated the performance of the proposed system in correcting the estimated position based on the given inputs.

As shown in the demonstrated results, the proposed new approach was able to provide excellent performance during the GPS signal outage or delay. For instance, figure 17 demonstrates the fused data along the x direction where two GPS signals outages or delays were detected during the drive test as shown by blue circles. As can be noticed, the proposed approach continued to estimate the position accurately in spite of the detected faults. The figure shows that the estimated position is in agreement with the solution fused by the MIDG.

The same approach was conducted for the data collected for both the y and z directions. The obtained results were plotted in figure 18a and 18b, along with the MIDG solution, using the open loop mode during the training phase for the y and z directions, respectively. As can be noticed from the residual subplots, the proposed system demonstrated an acceptable performance in correcting the estimated position based on the given inputs along these directions. The error histograms for the developed ANARX networks along the x, y and z directions are shown in figure 19. The mean value for the error with respect to the MIDG reference is 3.73×10^{-6} m in the x direction, 4.83×10^{-6} m in the y direction, and 2.31×10^{-6} m in the and z directions.

To characterize the performance of the propose algorithm, the ANARX approach is compared to another nonlinear intelligent system using neuro fuzzy system [5]. Both schemes take into account the possibly varying delay between the availability of GPS measurements in the fusion technique. The proposed approach was able to provide excellent performance during the GPS signal outage. As reported in [5] the error in the x, y, z directions with respect to the MIDG reference were -1.03×10^{-2} m, 1.82×10^{-2} m and -2.04×10^{-3} m, respectively. As can be seen from figure 19, the proposed approach demonstrates reduced the position error along the x, y, and z directions. The results obtained from the open loop mode for the estimated vehicle's three-dimensional position is demonstrated together in figure 20. As can be seen, the estimated path of the vehicle closely matches the reference

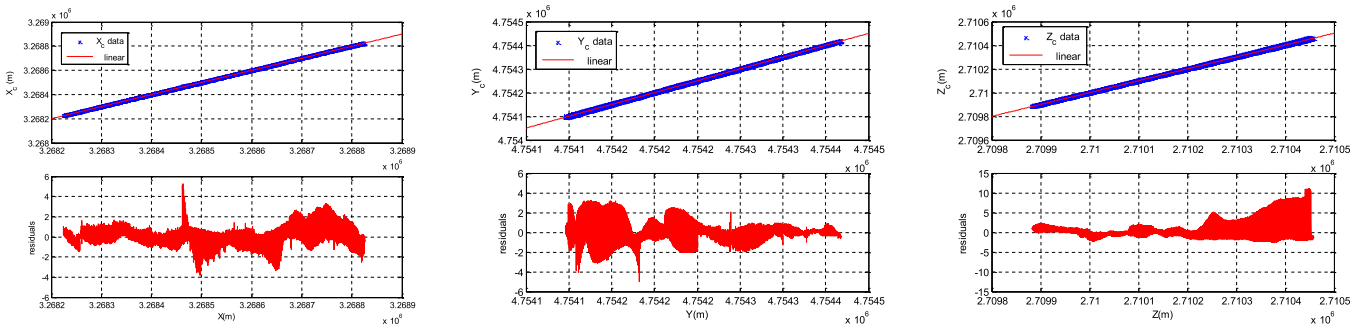

(a) (b) (c)

Fig. 23. The fused data scatter plot compared to the MIDG solution along the x, y, and z directions using closed loop ANARX model.

MIDG solution, shown in figure 15, throughout the path of vehicle motion.

For enhanced real-time validation, the closed loop mode was implemented based on the developed ANARX approach. Vehicle's position was estimated along the same path using the new mode. Figures 21 shows the results after applying the collected data to the closed loop mode in the x, y, and z directions, respectively, plotted compared to estimated vehicle position form the open loop mode. As demonstrated from the results, the proposed approach was able to provide excellent performance during the closed loop mode in spite of the GPS signal outage or delay throughout the path. The estimated path of the vehicle closely matches the reference MIDG solution throughout the path of the vehicle motion as in Figure 15. For instance, figure 22 demonstrates the fused data along the z direction where a GPS signal outage or delay was detected during the drive test as shown between the samples 10000-10020. As can be noticed, the proposed approach was able to perform in an acceptable way and overcome the detected faults, moreover the estimated position agreed later on with that fused by the MIDG solution.

The residual subplots in Figures 23 a, b, and c demonstrate the proposed system's performance in correcting the estimated position based on the given input using the closed loop model along x, y and z directions respectively. As can be seen from the figures, the closed loop mode was able to provide excellent performance during the GPS signal outage that is in agreement with the open loop mode.

VI. Conclusion

In this paper, a non-linear, autoregressive INS/GPS measurement fusion architecture is proposed. This non-linear architecture is utilized to obtain a high-accuracy vehicle position estimate by exploiting the possible large estimation error that is obtained by integrating the low-cost IMU measurements. In addition, the proposed method takes into account the possible time-varying delay between the IMU and GPS measurements due to operation in urban canyon environments. First, the method was verified in a simulation environment against a known vehicle trajectory. Subsequently, experimental tests were conducted to verify the performance of the proposed architecture against a commercial standalone COTs solution. The results demonstrated the accuracy of the proposed approach in providing position estimates that are in agreement with the reference solution both in the simulation and experimental environments. Additionally, the accuracy of the proposed approach in compensating for GPS signal outages was verified.

References

[1] J. N. Gross, Y. Gu, and M. B. Rhudy, "Robust UAV relative navigation with DGPS, INS, and peer-to-peer radio ranging," *IEEE Trans. Autom. Sci. Eng.*, vol. 12, no. 3, pp. 935–944, Jul. 2015, doi: 10.1109/TASE.2014.2383357.

[2] D. Scaramuzza *et al.*, "Vision-controlled micro flying robots: From system design to autonomous navigation and mapping in GPS-denied environments," *IEEE Robot. Autom. Mag.*, vol. 21, no. 3, pp. 26–40, Sep. 2014.

[3] B. J. Emran, M. Al-Omari, M. F. Abdel-Hafez, and M. A. Jaradat, "Hybrid low-cost approach for quadrotor attitude estimation," *J. Comput. Nonlinear Dyn.*, vol. 10, no. 3, p. 031010, 2014.

[4] M. K. S. Al-Sharman, M. F. Abdel-Hafez, and M. A. R. I. Al-Omari, "Attitude and flapping angles estimation for a small-scale flybarless helicopter using a Kalman filter," *IEEE Sensors J.*, vol. 15, no. 4, pp. 2114–2122, Apr. 2015.

[5] M. A. K. Jaradat and M. F. Abdel-Hafez, "Enhanced, delay dependent, intelligent fusion for INS/GPS navigation system," *IEEE Sensors J.*, vol. 14, no. 5, pp. 1545–1554, May 2014.

[6] J. Fang, L. Chen, and J. Yao, "An accurate gravity compensation method for high-precision airborne POS," *IEEE Trans. Geosci. Remote Sens.*, vol. 52, no. 8, pp. 4564–4573, Aug. 2014.

[7] C. Miao and J. Li, "Autonomous landing of small unmanned aerial rotorcraft based on monocular vision in GPS-denied area," *IEEE/CAA J. Automatica Sinica*, vol. 2, no. 1, pp. 109–114, Jan. 2015.

[8] M. Y. Zhong, J. Guo, and Q. Cao, "On designing PMI Kalman filter for INS/GPS integrated systems with unknown sensor errors," *IEEE Sensors J.*, vol. 15, no. 1, pp. 535–544, Jan. 2015.

[9] M. F. Abdel-Hafez, "On the development of an inertial navigation error-budget system," *J. Franklin Inst.*, vol. 348, no. 1, pp. 24–44, Feb. 2011.

[10] A. Nemra and N. Aouf, "Robust INS/GPS sensor fusion for UAV localization using SDRE nonlinear filtering," *IEEE J. Sensors*, vol. 10, no. 4, pp. 789–798, Apr. 2010.

[11] W. Jiang, Y. Li, and C. Rizos, "Optimal data fusion algorithm for navigation using triple integration of PPP-GNSS, INS, and terrestrial ranging system," *IEEE Sensors J.*, vol. 15, no. 10, pp. 5634–5644, Oct. 2015.

[12] M. F. Abdel-Hafez, "The autocovariance least-squares technique for GPS measurement noise estimation," *IEEE Trans. Veh. Technol.*, vol. 59, no. 2, pp. 574–588, Feb. 2010.

[13] A. D. Sarma, G. S. Rao, P. V. D. S. Rao, and K. Ramalingam, "GPS satellite and receiver instrumental biases estimation using SVD algorithm," *IEEE Trans. Aerosp. Electron. Syst.*, vol. 44, no. 4, pp. 1560–1566, Oct. 2008.

[14] M. F. Abdel-Hafez, "Detection of bias in GPS satellites' measurements: A probability ratio test formulation," *IEEE Trans. Control Syst. Technol.*, vol. 22, no. 3, pp. 1166–1173, May 2014.

[15] A. Noureldin, A. El-Shafie, and M. Bayoumi, "GPS/INS integration utilizing dynamic neural networks for vehicular navigation," *Inf. Fusion*, vol. 12, no. 1, pp. 48–57, 2011.

[16] J. Zhang, S. Singh, and G. Kantor, "Robust monocular visual odometry for a ground vehicle in undulating terrain," in *Field and Service Robotics*. Berlin, Germany: Springer, 2013, pp. 311–326.
[17] C. Barrios and Y. Motai, "Improving estimation of vehicle's trajectory using the latest global positioning system with Kalman filtering," *IEEE Trans. Instrum. Meas.*, vol. 60, no. 12, pp. 3747–3755, Dec. 2011.
[18] A. Bergeron and N. Baddour, "Design and development of a low-cost multisensor inertial data acquisition system for sailing," *IEEE Trans. Instrum. Meas.*, vol. 63, no. 2, pp. 441–449, Feb. 2014.
[19] S. Sukkarieh, "Low cost, high integrity, aided inertial navigation systems for autonomous land vehicles," Ph.D. dissertation, Dept. Mech. Mechatron. Eng., Austral. Centre Field Robot., Univ. Sydney, Sydney, NSW, Australia, 2000.
[20] T. Zhang and X. Xu, "A new method of seamless land navigation for GPS/INS integrated system," *Measurement*, vol. 45, no. 4, pp. 691–701, 2012.
[21] D. C. Salmon and D. M. Bevly, "An exploration of low-cost sensor and vehicle model Solutions for ground vehicle navigation," in *Proc. IEEE/ION Position, Location Navigat. Symp.-PLANS*, May 2014, pp. 462–471.
[22] E. D. Martí, D. Martín, J. García, A. de la Escalera, J. M. Molina, and J. M. Armingol, "Context-aided sensor fusion for enhanced urban navigation," *Sensors*, vol. 12, no. 12, pp. 16802–16837, 201.
[23] D. J. Jwo and S. H. Wang, "Adaptive fuzzy strong tracking extended Kalman filtering for GPS navigation," *IEEE Sensors J.*, vol. 7, no. 5, pp. 778–789, May 2007.
[24] M. F. Abdel-Hafez, "High integrity GPS/INS filter for precise relative navigation," Ph.D. dissertation, Dept. Mech. Aerosp. Eng., Univ. California, Los Angeles, CA, USA, 2003.
[25] Y. Bar-Shalom, X. R. Li, and T. Kirubarajan, *Estimation With Applications to Tracking and Navigation: Theory Algorithms and Software*, New York, NY, USA: Wiley, 2001.
[26] S. Sadhu, M. Srinivasan, S. Bhaumik, and T. K. Ghoshal, "Central difference formulation of risk-sensitive filter," *IEEE Signal Process. Lett.*, vol. 14, no. 6, pp. 421–424, Jun. 2007.
[27] P. Setoodeh, A. R. Khayatian, and E. Farjah, "Attitude estimation by divided difference filter-based sensor fusion," *J. Navigat.*, vol. 60, no. 1, pp. 119–128, 2007.
[28] J. Rezaie, B. Moshiri, B. N. Araabi, and A. Asadian, "GPS/INS integration using nonlinear blending filters," in *Proc. Annu. Conf. (SICE)*, Sep. 2007, pp. 1674–1680.
[29] J.-S. Kim, S. Yoon, and D.-R. Shin, "A state-space approach to multiuser parameters estimation using central difference for CDMA systems," *Wireless Pers. Commun.*, vol. 40, pp. 457–478, 2007.
[30] R. Dutta and A. Terhorst, "Adaptive neuro-fuzzy inference system-based remote bulk soil moisture estimation: Using CosmOz cosmic ray sensor," *IEEE Sensors J.*, vol. 13, no. 6, pp. 2374–2381, Jun. 2013.
[31] M. A. K. Jaradat and R. Langari, "A hybrid intelligent system for fault detection and sensor fusion," *Appl. Soft Comput.*, vol. 9, no. 1, pp. 415–422, 2009.
[32] N. B. Hui, V. Mahendar, and D. K. Pratihar, "Time-optimal, collision-free navigation of a car-like mobile robot using neuro-fuzzy approaches," *Fuzzy Sets Syst.*, vol. 157, no. 16, pp. 2171–2204, 2006.
[33] A. Noureldin, A. El-Shafie, and M. R. Taha, "Optimizing neuro-fuzzy modules for data fusion of vehicular navigation systems using temporal cross-validation," *Eng. Appl. Artif. Intell.*, vol. 20, no. 1, pp. 49–61, 2007.
[34] N. El-Sheimy, K. W. Chiang, and A. Noureldin, "The utilization of artificial neural networks for multisensor system integration in navigation and positioning instruments," *IEEE Trans. Instrum. Meas.*, vol. 55, no. 5, pp. 1606–1615, Oct. 2006.
[35] C. M. Bishop, *Neural Networks for Pattern Recognition*. New York, NY, USA: Oxford Univ. Press, 1995.
[36] J.-S. R. Jang, "ANFIS: Adaptive-network-based fuzzy inference system," *IEEE Trans. Syst., Man, Cybern.*, vol. 23, no. 3, pp. 665–685, May/Jun. 1993.
[37] M. Negnevitsky, *Artificial Intelligence: A Guide to Intelligent Systems*, 3rd ed. Reading, MA, USA: Addison-Wesley, 2011.
[38] K. Saadeddin, M. F. Abdel-Hafez, M. A. Jaradat, and M. A. Jarrah, "Optimization of intelligent approach for low-cost INS/GPS navigation system," *J. Intell. Robot. Syst.*, vol. 73, no. 1, pp. 325–348, 2014.
[39] Omni Instruments Ltd. (2015). [Online]. Available: http://www.omniinstruments.co.uk/gyro/MIDGII.htm
[40] E. Petlenkov, S. Nomm, and U. Kotta, "Neural networks based ANARX structure for identification and model based control," in *Proc. 9th Int. Conf. Control, Autom., Robot. Vis., (ICARCV)*, vol. 6, Dec. 2006, pp. 1–5.
[41] S. Nomm and U. Kotta, "Comparison of neural networks-based ANARX and NARX models by application of correlation tests," in *Proc. Int. Joint Conf. Neural Netw. (IJCNN)*, Jul. 2011, pp. 2113–2118.
[42] Mathworks. (2015). *Matlab Neural Network Tool Box*. [Online]. Available: http://www.mathworks.com

Mohammad Abdel Kareem Jaradat received the B.Sc. degree from Jordan University of Science & Technology, Jordan, and the M.Sc. and Ph.D. degrees in mechanical engineering from Texas A&M University, College Station, TX, USA. Currently, he is an Associate Professor with American University of Sharjah, and with the Jordan University of Science & Technology. During his integrated experience several projects, prototypes and publications are conducted, specialized on the following research areas: robotics, artificial intelligent systems, mechatronics system design, sensor fusion, fault diagnostics, intelligent nanosystems, intelligent control, and embedded control systems.

Mamoun F. Abdel-Hafez received the B.S. degree in mechanical engineering from the Jordan University of Science and Technology in 1997, the M.S. in mechanical engineering from the University of Wisconsin, Milwaukee, in 1999, and the Ph.D. degree in mechanical engineering from the University of California at Los Angeles (UCLA) in 2003. He is currently with the Department of Mechanical Engineering, American University of Sharjah. He served as a Post-Doctoral Research Associate with the Department of Mechanical and Aerospace Engineering, UCLA, from 2003 to 2003, where he was involved in a research project on fault-tolerant autonomous multiple aircraft landing. His research interests are in stochastic estimation, control systems, sensor fusion and fault detection.